Comparison of Measurement and Modeling of Current Profile Changes due to Neutral Beam Ion Redistribution during TAE Avalanches in NSTX*)

Douglass S. DARROW, Neal CROCKER1), Niklolai N. GORELENKOV, Shigeyuki KUBOTA1),
Mario PODESTÀ, Lei SHI and Roscoe WHITE

Princeton Plasma Physics Laboratory, PO Box 451, Princeton, NJ 08453-0451, USA
1)*Department of Physics, University of California, Los Angeles, Los Angeles, CA, USA*

(Received 9 December 2012 / Accepted 22 April 2013)

Brief 'avalanches' of toroidal Alfvén eigenmodes (TAEs) are observed in NSTX plasmas with several different n numbers simultaneously present. These affect the neutral beam ion distribution as evidenced by a concurrent drop in the neutron rate and, sometimes, beam ion loss. Guiding center orbit modeling has shown that the modes can transiently render portions of the beam ion phase space stochastic. The resulting redistribution of beam ions can also create a broader beam-driven current profile and produce other changes in the beam ion distribution function.

Keywords: Toroidal Alfvén eigenmode, neutral beam ion loss, beam driven current, guiding center orbit, orbit stochasticity

DOI: 10.1585/pfr.8.2402119

1. Introduction

Avalanches consisting of brief bursts composed of TAEs [1] of several different toroidal mode numbers, n, are sometimes seen in NSTX plasmas [2]. These typically cause a drop in the neutron rate and sometimes a measurable loss of neutral beam ions [3]. Detailed guiding center orbit modeling of these events has been performed and indicates that the beam ion losses can be attributed to mode-driven stochastization [4] of the beam ion orbit phase space. Similar interactions between ICRF heated tail ions and MHD modes in the ASDEX-Upgrade device have also been observed, with similar conclusions about the underlying mechanisms of fast ion transport [5], and signatures of stochastic loss of beam ions have also been seen in Compact Helical System plasmas [6].

Ohmic drive of plasma current in spherical tokamaks (STs) is typically quite limited due to the small cross sectional area of the transformer primary windings necessitated by the desire to minimize the plasma aspect ratio. Consequently, neutral beam injection in such plasmas is as important for current drive as it is for plasma heating. Given this, any plasma event which alters the beam ion distribution function substantially is of concern not only for the wall heat loads and changes in plasma heating it may engender, but also for effects it may have on the beam driven current. This issue of mode-induced effects on the beam-driven current profile has been little considered as yet. Here some initial results are presented on this topic.

2. Method

As an initial example, an avalanche in NSTX shot 141719 at 383 ms is used. This event and its analysis with the guiding center orbit code ORBIT [4,7] are documented in Ref. 3. To summarize briefly here, this discharge had $I_\mathrm{p} = 0.9\,\mathrm{MA}$, $B_0 = 0.54\,\mathrm{T}$, with one neutral beam source injecting 2 MW of 90 kV D atoms and a second source injecting 0.5 MW of 50 kV D^0. The avalanche had TAEs with $n = 1$, 2, 3, and 4 present and it lasted for ~2 ms. The neutron rate dropped by 17 percent over the course of the avalanche, and a scintillator type fast ion loss probe [8] observed both passing and trapped beam ion losses. TAE mode structures from NOVA-K were scaled to fit displacements observed by a multichannel microwave reflectometer system [9] and these modes were input into ORBIT. The ORBIT simulation for this case followed a population of 180,000 newly-injected 90 keV D ions, whose deposition was calculated by TRANSP [10]. Orbits were followed in the equilibrium plus TAE fields. The computed loss beam ion distribution at the probe also consisted of passing and trapped ions, though the pitch angle range of the modeled loss did not coincide precisely with the observations.

Given the ORBIT code initial and final particle distributions, it is possible to construct the model beam-driven current profile both before and after the avalanche to determine the effect of this event on the profile. To do this, the beam ion current density ($\Sigma nqv_\parallel$) is tabulated as a function of flux surface. Figure 1 displays the profiles before and after the avalanche. Note that the current densities shown are only those carried in the beam ions and they do

---

author's e-mail: ddarrow@pppl.gov

*) This article is based on the presentation at the 22nd International Toki Conference (ITC22).

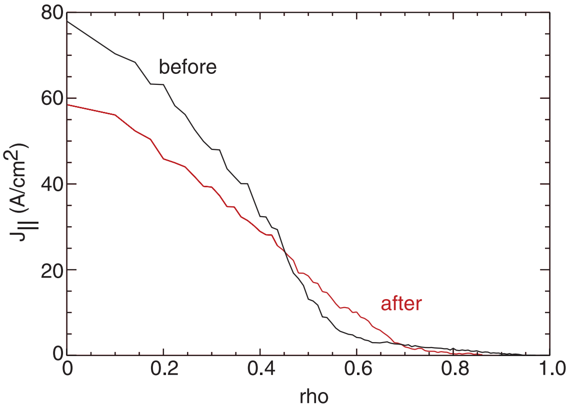

Fig. 1 Current density profile in the neutral beam ions before and after the avalanche. Note that avalanche enhances the current density outward of the half-radius and lowers central current density.

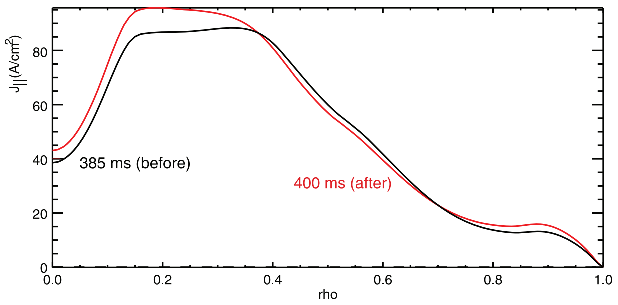

Fig. 2 Current density profiles before and after the avalanche, as taken from LRDFIT equilibrium fits, constrained by MSE measurements.

not account for any electron screening of the beam ions, which would likely diminish the current densities shown. The principal effects of the avalanche are to decrease the on-axis current density and also increase it over the range $0.45 \leq r/a \leq 0.75$. The additional current density at larger minor radii is a robust result, appearing at multiple grid points. This indicates that avalanches can broaden the current profile, an effect that may be useful in sustaining reversed q shear profiles.

Figure 2 shows the current profiles from MSE-constrained plasma equilibrium fits before and after the avalanche. These show some similarities and differences from the modeled changes in current profile. In contrast to the model, they show an increase in the central current density after the avalanche, but they agree on an increase in the current density in the outer region of the plasma. However, the region where the equilibrium fits show a change in profile are different from where the model results show a change. Ultimately, the equilibrium fits are unlikely to have the fitting accuracy to distinguish changes in current density of the level produced in the model.

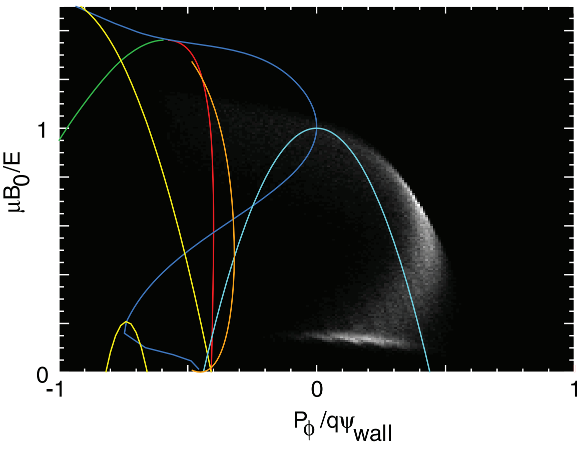

Fig. 3 Deposited 90 keV D beam ion distribution before avalanche, as computed by TRANSP. Each point in this plane represents a single orbit, and the intensity black-to-white indicates the relative abundance of particles on that orbit. The horizontal axis is normalized canonical toroidal momentum and the vertical axis is normalized magnetic moment. The light blue curve is the locus of all guiding centers passing through the magnetic axis, the large yellow parabola comprises all guiding centers reaching the outer midplane, the small yellow parabola is all guiding centers reaching the inner midplane wall, the dark blue curve is the passing/trapped boundary. The red/green curve is the boundary for loss of particles to the wall and the orange curve is the scintillator loss detector.

3. 90 keV Beam Ion Phase Space

In the avalanche being considered, the lost beam ions all appeared to be at 90 keV. Consequently, it is reasonable to limit consideration of the effect of the modes to only particles at or very close to this energy. Since guiding center orbits in an axisymmetric tokamak for particles of a given mass and charge are fully determined by knowing their energy, magnetic moment, and canonical toroidal momentum, this simplification reduces the beam ion phase space to two dimensions. Figure 3 shows the initial distribution of newly deposited 90 keV beam ions used in the ORBIT simulations, along with certain boundaries in the phase space. The deposition consists essentially entirely of passing particles in two distinct concentrations, one at very parallel velocities and the second at somewhat more perpendicular but still passing trajectories.

Within the phase space domains that are rendered stochastic during the presence of the TAEs, particles can be convected along lines described by $nE - \omega P_\phi = const$. The frequencies and wavelengths of the TAEs are such that they do not alter the magnetic moment of the beam ions. In practice, the effect of the modes is to transport the beam ions in P_ϕ with a change in energy that is less than 10 percent. Hence, in the phase space plot of Fig. 3, particle motion is exclusively horizontal, with changes in energy that can be considered displacement to a plane parallel to that shown. When particles are transported to the right in this

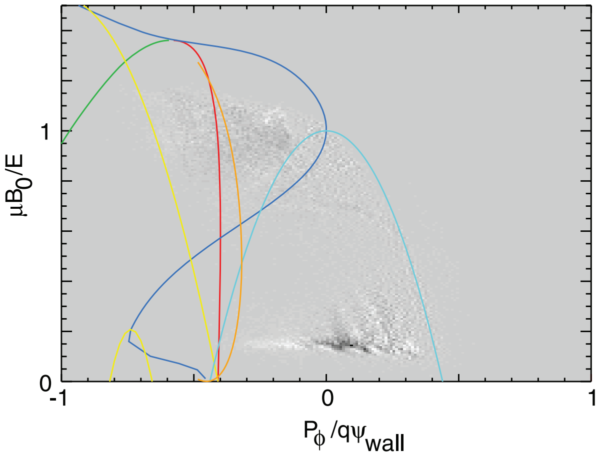

Fig. 4 The difference in the 90 keV beam ion distribution function arising from the avalanche (final minus initial distribution). Dark regions indicate depletion of particles by the avalanche and lighter regions indicate an accumulation of particles.

phase space representation, they remain confined. Transport to the left, however, can result in the particle being lost, if it reaches the loss boundary (red curve).

Given that the initial and final particle distributions from the ORBIT run are known, it is also possible to create a plot of the changes the avalanche has wrought in the distribution function. That result is shown in Fig. 4, as the final distribution minus the initial distribution over the same domain depicted in Fig. 3. In this figure, regions where the final distribution is depleted relative to the initial appear darker, while areas of greater particle concentration after the avalanche appear whiter. This figure shows a diffuse depletion of trapped particles with normalized magnetic moment near unity. At low magnetic moemtn (i.e. pitch angle) localized stronger depletion is observed, with also some accumulation of particles. At normalized mu~0.2, there is evidence of depletion of a population just above $P_\phi = 0$, with accumulation just below $P_\phi = 0$. This is consistent with the notion just mentioned of roughly horizontal transport in this plane.

In conclusion, beam ion orbit modeling during a TAE avalanche has shown evidence of a broadened beam driven current profile after the avalanche, with loss and redistribution of some of the beam population.

This work supported by US DoE contracts DE-ACO2-09CH11466 and DE-FG-99ER54527.

[1] C. Cheng and M. Chance, Phys. Fluids **29**, 3695 (1986).

[2] E. Fredrickson *et al.*, Phys. Plasmas **16**, 122505 (2009).

[3] D. Darrow *et al.*, to appear in Nucl. Fusion (2013).

[4] R. White, Comm. Nonlinear Science Numerical Simulations **17**, 2200 (2012).

[5] M. García-Muñoz *et al.*, Nucl. Fusion **50**, 084004 (2010).

[6] K. Shinohara *et al.*, Plasma Fusion Res. **2**, 042 (2007).

[7] R. White and M. Chance, Phys. Fluids **27**, 2455 (1984).

[8] D. Darrow, Rev. Sci. Instrum. **79**, 023502 (2008).

[9] N. Crocker *et al.*, Plasma Phys. Control. Fusion **15**, 105001 (2011).

[10] R. Hawryluk, in 1980 *Physics of Plasmas Close to Thermonuclear Conditions*, vol 1 ed Coppi B *et al.* (CEC:Brussels, 1980) p.19.